Available online at www.sciencedirect.com
ScienceDirect
Journal of Environmental Sciences 19(2007) 1505–1509
JOURNAL OF ENVIRONMENTAL SCIENCES
ISSN 1001-0742
CN 11-2629/X
www.jesc.ac.cn

Characterization of metal doped-titanium dioxide and behaviors on photocatalytic oxidation of nitrogen oxides

LIU Yue, WANG Hai-qiang, WU Zhong-biao*

Department of Environmental Engineering, Zhejiang University, Hangzhou 310027, China. E-mail: yueliu@zju.edu.cn

Received 2 March 2007; revised 2 April 2007; accepted 23 April 2007

Abstract

A series of nanosized ion-doped TiO_2 catalysts with different ion content (between 0.1 at.% and 1.0 at.%) have been prepared by wet impregnation method and investigated with respect to their behavior for UV photocatalytic oxidation of nitric oxide. The catalytic activity was correlated with structural, electronic and surface examinations of the catalysts using X-ray diffraction analysis (XRD), ultraviolet-visible (UV-Vis) absorption spectroscopy, transmission electron microscopy (TEM), energy disperse spectrometer (EDS) and high resolution-transmission electron microscopy (HR-TEM) techniques. An enhancement of the photocatalytic activity was observed for Zn^{2+} doping catalyst ranged from 0.1 at.% to 1.0 at.% which was attributed to the lengthened lifetime of electrons and holes. The improvement in photocatalytic activity could be also observed with the low doping concentration of Cr^{3+} (0.1 at.%). However, the doping of Fe^{3+}, Mo^{6+}, Mn^{2+} and the high doping concentration of Cr^{3+} had no contribution to photocatalytic activity of nitric oxide.

Key words: NO; photocatalytic oxidation; ion doping; doped

Introduction

The worsening of one's living environment due to nitrogen oxides (NO_x) has constituted a serious social problem. NO_x has caused various environmental problems. It is well known that NO_x cause acid rain and photochemical smog (Castro *et al*., 2001; Farrell, 2001). Various processes, including combustion improving, dry processes and wet processes have been developed to remove NO from flue gas (Radojevic, 1998; Efstathiou and Fliatoura, 1995; Heck, 1999).

Wet processes are very efficient to remove NO_2 from flue gas, but cannot remove NO because of its low solubility in aqueous solution (Takeuchi *et al*., 1977; Chen *et al*., 2002). One promising approach to improve the absorption efficiency of wet processes is the transformation of NO to NO_2 by photocatalytic oxidation (PCO).

The PCO of NO_x in ambient atmosphere, using TiO_2 as the photocatalyst, was first reported in 1994 (Ibusuki and Takeuchi, 1994). The mechanism for the PCO of NO was then studied (Devahasdin *et al*., 2003; Dalton *et al*., 2002). It was found that, the PCO behavior consisted of a series of oxidation steps with OH· radical and O_2^- involved. Furthermore, the catalysts just like TiO_2 sheets that contained metal compounds (Ichiura *et al*., 2003), TiO_2-zeolite composite catalyst (Hashimoto *et al*., 2001), and titania with NH_3 pretreatment were also studied (Li *et al*., 2004).

Unfortunately, the mentioned investigations are mostly focus on the removal of NO from ambient environment (either indoor or outdoor air). Comparing with NO_x from flue gas, the concentration of NO from ambient environment is much lower. Therefore, it is necessary to develop more effective ways to enhance the photocatalytic efficiency at high concentration of NO for the treatment of NO from flue gas.

An alternative approach to modifying the photoreactivity of the TiO_2 particle is to dope it with metal ions to restrain electron-hole recombination. This approach had also been investigated extensively using a range of transition metal ions (Fe, V, Cr, Mn, Cu, Co, Mo etc.) in connection with the use of TiO_2 particles to effect the photomineralisation of pollutants (Kemp and McIntyre, 2006; Litter and Navío, 1996; Navío *et al*., 1999; Yang *et al*., 2004; Zhou *et al*., 2005; Kapoor *et al*., 2005).

This article mainly focused on the investigations on the photocatalytic activity and characterization of titanium dioxide powder doped with transition metal. The doped titanium dioxide powders were characterized by X-ray diffraction analysis (XRD), ultraviolet-visible (UV-Vis) absorption spectroscopy, transmission electron microscopy (TEM), energy disperse spectrometer (EDS) and high resolution-transmission electron microscopy (HR-TEM) techniques. The photoactivity for the oxidation of nitrogen

Porject supported by the New Century Excellent Scholar Program of Ministry of Education of China (No. NCET-04-0549) and the China Postdoctoral Science Foundation (No. 20060401047). *Corresponding author. E-mail: zbwu@zju.edu.cn.

oxides of the doped catalysts was tested, the relationship between the doped transition metal ions and NO oxidation efficiency was discussed.

1 Experimental

1.1 Preparation of TiO_2 catalysts

The Degussa P25 TiO_2 powder (crystal size: 30–50 nm, surface area: 50±5 m^2/g, Degussa Co. Ltd., Germany) was used to prepare the TiO_2 catalysts that contained 0.1, 0.5, and 1.0 moles of metal ions over 100 moles of titanium ions by the wet impregnation method (Paola *et al*., 2002). The chemicals of $Zn(NO_3)_2{\cdot}6H_2O$, $Fe(NO_3)_3{\cdot}9H_2O$, $Cr(NO_3)_3{\cdot}9H_2O$, $(NH_4)_6Mo_7O_{24}{\cdot}4H_2O$, $Mn(NO_3)_2$ used as the precursors was analytical grade. TiO_2 powder was impregnated with aqueous solutions containing the required amounts of the transition metal ions, and then kept at room temperature for 24 h.

Immobilization was carried out by the dip-coating method. The catalyst suspension, i.e. TiO_2 powder doped with transition metal, was gradually dropped and was coated on the woven glass fabric (pretreatment at 500°C for 1 h) over an area of 4 cm × 80 cm. The coated woven glass fabric was treated with a desiccation process in a convection oven at 80°C overnight and then calcinated at 400°C for 1 h. The amount of TiO_2 imposed was determined as the mass increase of the woven galss fabric after the coating. In all experiments, the weight of TiO_2 coated was determined to be 0.5 g ± 10%.

1.2 Characterization of TiO_2 catalysts

XRD of the catalysts was performed on a difractometer (D/Max RA, Rigaku, Japan) at 40 kV and 150 mA, at an angle of 2θ from 20 to 80°. The morphology, structure and grain size of TiO_2 particle were examined by TEM and HR-TEM using a JEM-2010 instrument (JEOL Co., Ltd., Japan). Particle surfaces and chemical compositions were characterized using a JEM-2010 TEM connected to an Oxford EDS. Diffuse absorbance spectra were recorded by means of a Purkinje TV-1901 instrument, using $BaSO_4$ as reference sample.

1.3 Experimental setup

A series of experiments for the removal of NO from a gaseous phase was carried out in the continuous-flow reactor using the catalysts prepared under different conditions. The schematic experimental setup consisted of the gas supply, PCO reactor, and analytical system (Wang *et al*., 2007). The air, NO, and N_2 gas streams were mixed to obtain the desired concentration (NO_x: 90 ppmv; NO: 80 ppmv; relative humidity: 80%). The flow rate of the gas was 2.0 L/min and the empty bed retention time (EBRT) was 10 s. After a stabilized period of about 1 h, there is no difference between outlet NO concentration and that of inlet gas, and then the experiment started by turning on the UV lamp.

NO, NO_2 and O_2 were measured with a Kane International Limited Model KM-9106 flue gas analyzer. The relative humidity was measured with a relative humidity analyzer (Model 605-H1, Testo Co. Ltd., China). The NO conversion (R_{NO}) is evaluated according to the definition as:

$$R_{NO} = (C_{NO_{inlet}} - C_{NO_{outlet}}) / C_{NO_{inlet}} \times 100\% \quad (1)$$

2 Result and discussion

2.1 Photocatalytic oxidation of NO

The PCO behavior was studied using Degussa P25 as photocatalyst (Fig.1). It consisted of a series of oxidation steps by the OH· radical and O_2^-: NO ⟶ HNO_2 ⟶ NO_2 ⟶ HNO_3 (Devahasdin *et al*., 2003; Wang *et al*., 2007). Obviously, the concentration of NO dropped rapidly and reached a steady state at the outlet after 30 min. The PCO of NO produces two major products: NO_2 in gas phase and HNO_3 on catalyst surface. At steady state, the equilibrium between HNO_3 and NO_2 was reached on the catalyst surface. NO_2 was the dominant product at the steady state. In this experiment, the steady state was defined as the situation after 120 min reaction, since the variation of the outlet concentration of the NO was less than 5%.

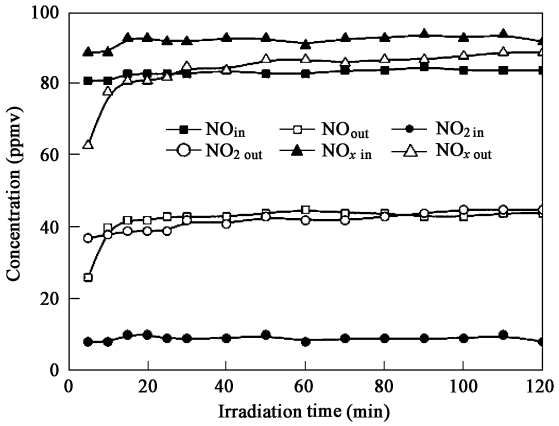

Fig. 1 Photocatalytic behavior of nitric oxide. 125 W Hg-arc lamp; relative humidity: 60%; EBRT: 10 s; O_2 concentration: 21%; catalyst: Degussa P25.

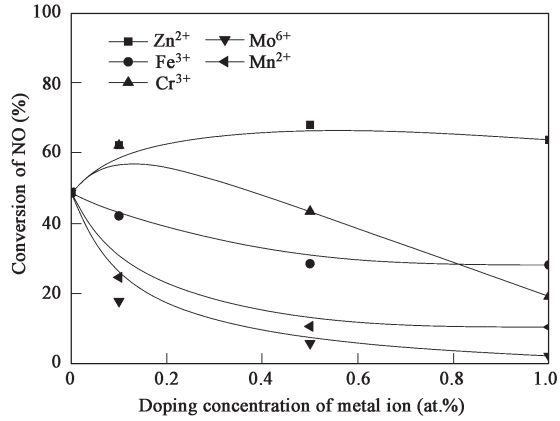

Fig. 2 NO conversion efficiency of catalysts with different ion doping. 125 W Hg-arc lamp; relative humidity: 80%; O_2 concentration: 21%; EBRT: 10 s.

2.2 Photocatalytic activity of ion doped catalysts

The conversion of NO over the ion doped catalysts at steady state is shown in Fig.2. It shows that Zn^{2+} doping could improve the photocatalytic oxidation activity of NO with the doping concentration ranged from 0.1 at.% to 1.0 at.%. The best photocatalytic activity was obtained with 0.5 at.% Zn^{2+} doping, which was nearly 20% higher than the pure Degussa P25. The photocatalytic activity of Cr^{3+} doped catalysts could be improved at a low doping concentration (0.1 at.%). However, the photocatalytic activity decreased fast with an increase of Cr^{3+} doping concentration. The effect of doping concentration of Fe^{3+}, Mo^{6+} and Mn^{2+} ions on the NO conversion is also shown in Fig.2. The results indicated that photocatalytic activity of the doped photocatalysts (Fe^{3+}, Mo^{6+}, and Mn^{2+}) decreased remarkably compared with the pure Degussa P25.

2.3 Crystal structure and size of ion doped TiO_2 catalysts

The XRD photographs of the Fe^{3+}-TiO_2 catalyst with different doping concentrations were presented in Fig.3. The anatase crystal sizes of these catalysts, determined by the Scherrer equation, ranged from 20 to 25 nm. And the rutile crystal sizes were within the range between 50 and 60 nm. It was found that the cystal size of doped catalysts had little change with the pure Degussa P25 particles.

From the X-ray diffraction, it could be seen that with different doping concentration (0.1 at.%–1.0 at.%), none of the XRD spectra gave intense peaks for ferric oxides. It could be due to the high dispersion and/or low crystalline nature of the ferric oxides on the titanium dioxide.

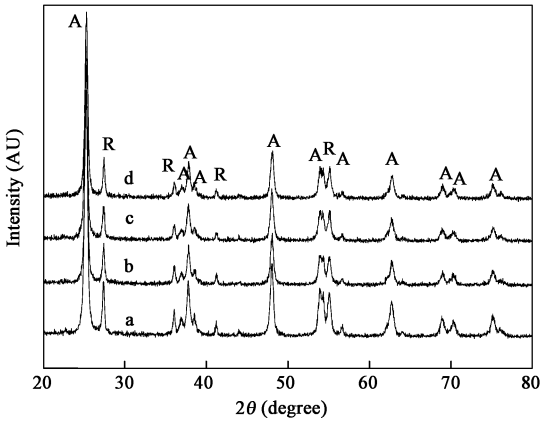

Fig. 3 XRD patterns of Fe^{3+} doped TiO_2 catalysts with different doping concentration. (a) Degussa P25; (b) 0.01 at.% Fe^{3+}; (c) 0.05 at.% Fe^{3+}; (d) 1.0 at.% Fe^{3+}.

2.4 Microstructure and crystallization analysis by TEM and HR-TEM

TEM and HR-TEM were used to study the microstructures and crystallization of the ion doped TiO_2 powders. TEM and HR-TEM micrographs of Zn^{2+} doped TiO_2 particles are shown in Fig.4. The TEM micrograph of Zn^{2+}-TiO_2 (Fig.4a) shows that the primary particle sizes were in the range from 20 to 50 nm, which were in agreement with the value of the crystallite size determined by XRD spectra. Furthermore, it could not found special particles for the zinc oxides. It was confirmed that Zn^{2+} was well dispersed in the TiO_2 particle. Fig.4b shows the HR-TEM image of Zn^{2+} doped TiO_2 particles. From Fig.4b clear lattice fringes could be observed, which allowed the identification of crystallographic spacing and indicated the ion doping had little influence on the crystal structure of TiO_2.

The EDS spectra of Zn^{2+} doped TiO_2 are shown in Fig.5, and the elements content are shown in Table 1. It is clearly shown that Zn^{2+} was well dispersed in the TiO_2 particles. The C element was contributed to the impurity of TiO_2, and the Cu element was contributed to the copper-net support used in the TEM analysis. And the calculated Zn^{2+} content in the TiO_2 particle was 0.43 at.%, which agreed well with the designed doping concentration.

2.5 UV-Vis analysis

UV-Vis spectroscopy has been widely used to investigate the band structure of TiO_2. The absorption spectra of TiO_2 powders with different ion doping are shown in

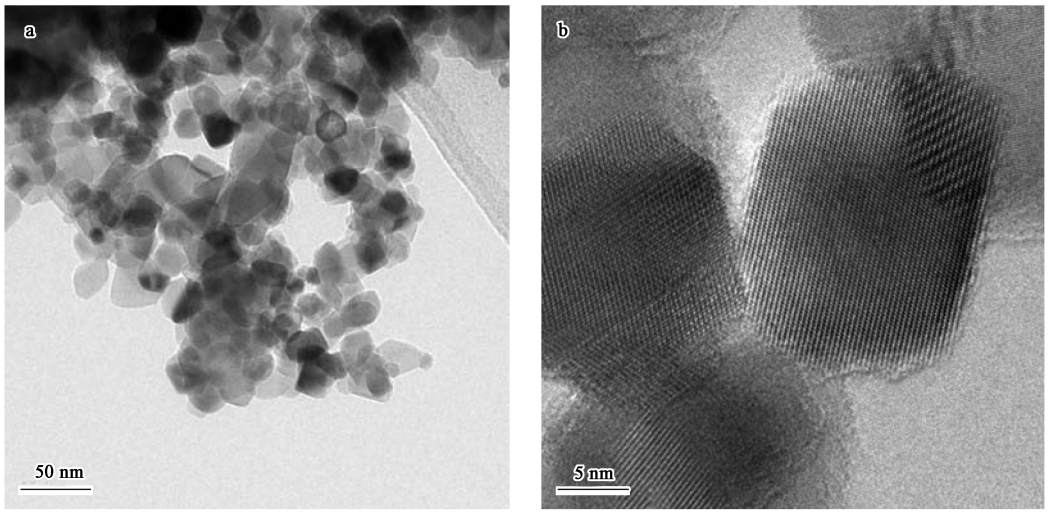

Fig. 4 TEM and HR-TEM micrographs of Zn^{2+} doped TiO_2 particles. (a) TEM of 0.5 at.% Zn^{2+} doped TiO_2 particles; (b) HR-TEM of 0.5 at.% Zn^{2+} doped TiO_2 particles.

Table 1 Element content of EDS (0.5 at.% Zn^{2+} doped TiO_2 particles)

Element	Peak area	Weight (%)	Atomic content (at.%)
C	401	4.32	11.06
O	2723	24.07	46.27
Ti	9898	50.73	32.57
Cu	3022	20.16	9.76
Zn	102	0.71	0.34
Total		100.00	

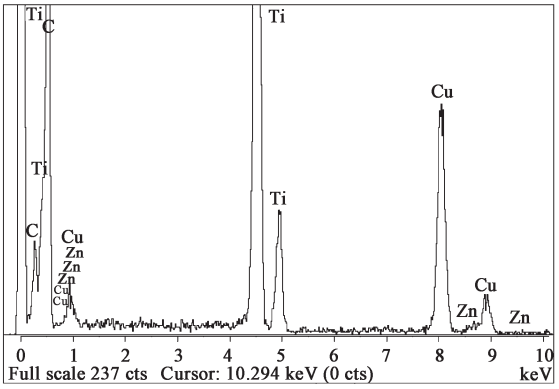

Fig. 5 EDS spectra of 0.5 at.% Zn^{2+} doped TiO_2 particles.

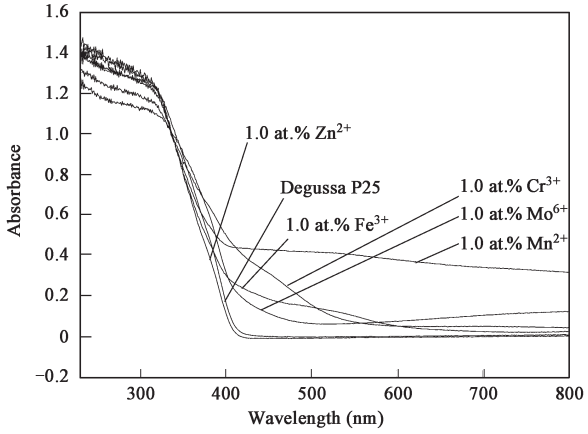

Fig. 6 UV-Vis absorbance spectra for the ion doped titania powder.

Fig.6. Inspection of the UV-Vis spectra for the different products (Fig.6) clearly indicated that Fe^{3+}, Mo^{6+}, and Mn^{2+} components had stronger visible absorption in the range of 450–650 nm. A similar visible absorption behavior had been observed for the Fe^{3+} doped titania (Piera *et al*., 2003), the Cr^{3+} doped titania (Zhu *et al*., 2006), the Mo^{6+} doped titania (Yang *et al*., 2004) and also for the Mn^{2+} doped titania (Dvoranová *et al*., 2002). It was noted that in the case of Zn^{2+}, the absorption edge was moved below 350 nm as compared to that of Degussa P25 TiO_2 (Kapoor *et al*., 2005).

3 Discussion

From the experimental results about the photocatalytic activities of M/TiO_2 catalysts (M = Zn, Fe, Cr, Mo, and Mn) for the gas phase oxidation of nitric oxide, it was found that only Zn^{2+} doping and Cr^{3+} doping with low concentration could improve the photocatalytic activity. In spite of the strong visible absorption shown by the Fe sample, it did not show any improvement in photocatalytic activity under UV-Vis. Also, the Mo^{6+}, Mn^{2+} doped titania particles were found to have much lower activity compared to pure Degussa P25 TiO_2.

In recent years, ion doping had been widely performed by chemical synthesis and other methods to improve photoactivity of titania (Kemp and McIntyre, 2006; Litter and Navío, 1996; Navío *et al*., 1999; Yang *et al*., 2004; Zhou *et al*., 2005; Kapoor *et al*., 2005). Because transition metal elements had many valences and trace transition metal ions doped in the TiO_2 matrix could be superficial potential trap of photogenerated electron-hole pairs, then lengthened the lifetime of electrons and holes and increased photocatalytic activity. But the previous study targets were almost aimed at VOCs, no study was concerned with the oxidation of nitric oxide. In the research carried out by Wu and Cheng (2006), it was found that nitric oxide was adsorbed on TiO_2 and M/TiO_2 in the form of bidentate nitrites and nitrates by reacting with OH groups, peroxo, or M=O species. In addition, NO could also be adsorbed on M^{n+} in the form of nitrosyls. Under UV irradiation, bidentate nitrite was oxidized to either monodentate or bidentate nitrate. Such oxidation was suggested to be induced by superoxo species generated by oxidizing peroxo species via photogenerated holes. The existence of nitrosyls deferred the oxidation of nitrites to nitrates due to the prior oxidation of nitrosyls by superoxo. Consequently, the oxidation rate of nitrites to nitrates had a significantly decrease in Cu/TiO_2, V/TiO_2 and Cr/TiO_2. These results could explain that the photocatlytic activity decrease with the doping of Fe^{3+}, Cr^{3+}, Mo^{6+} and Mn^{2+} ions on the TiO_2 particles. However, in our experiment, the low doping concentration (0.1 at.%) with Cr^{3+} could improve the photocatalytic activity of nitric oxide. It could not explain well by using Wu's theory (Wu and Cheng, 2006). ZnO was a semiconductor oxide which had the same energy band gap (3.2 eV) and similar electronic properties as TiO_2, but it had limited applications as a photocatalyst for the oxidative degradation purpose due to its photocorrosion (Pal and Sharon, 2002). In this study, the Zn^{2+} doped TiO_2 particles had a higher activity than the pure Degussa P25. That might be contributed to the lengthened lifetime of electrons and holes, which resulted in the improvement on photocatalytic activity of nitric oxide.

4 Conclusions

A series of nanosized iron-doped (Zn^{2+}, Fe^{3+}, Cr^{3+}, Mo^{6+}, Mn^{2+}) TiO_2 catalysts with different iron contents (between 0.1 at.% and 1.0 at.%) have been prepared by a wet impregnation method and examined with respect to their activity for photocatalytic oxidation of nitric oxide. The effects of ion and doping concentration on the TiO_2 particle characters and NO conversion efficiency were studied. It could be drawn from this study as:

For the Zn^{2+} doping ranged from 0.1 at.% to 1.0 at.%, an enhancement of the photocatalytic activity was observed. The best photocatalytic activity was obtained with 0.5

at.% Zn^{2+} doping, which was nearly 20% higher than the pure Degussa P25. It could be attributed to the lengthened lifetime of electrons and holes.

The photocatalytic activity of Cr^{3+} doped catalysts was improved a lot with low doping concentration (0.1 at.%). However, the photocatalytic activity decreased fast with an increase in Cr^{3+} doping concentration.

Compared with the pure Degussa P25, the photocatalytic activity of ion doped photocatalysts (Fe^{3+}, Mo^{6+}, and Mn^{2+}) decreased remarkablely. The doping of Fe^{3+}, Mo^{6+} and Mn^{2+} ions on the TiO_2 particle had no contribution to the photocatalytic activity of nitric oxide.

With the doping of Fe^{3+}, Cr^{3+}, Mo^{6+}, Mn^{2+}, NO could be adsorbed on M^{n+} in the form of nitrosyls. The existence of nitrosyls deferred the oxidation of nitrites to nitrates due to the prior oxidation of nitrosyls by superoxo. Thus, the oxidation rate of nitric oxide decreased significantly.

References

Castro T, Madronich S, Rivale S *et al*., 2001. The influence of aerosols on photochemical smog in Mexico city[J]. Atmos Environ, 35: 1765–1772.

Chen L, Lin J W, Yang C L, 2002. Absorption of NO_2 in a packed tower with Na_2SO_3 aqueous solution[J]. Environ Prog, 21: 225–230.

Dalton J S, Janes P A, Nicholson J A *et al*., 2002. Photocatalytic oxidation of NO_x gases using TiO_2: a surface spectroscopic approach[J]. Environ Pollut, 120: 415–422.

Devahasdin S, Fan C, Jr Li K *et al*., 2003. TiO_2 photocatalytic oxidation of nitric oxide: transient behavior and reaction kinetics[J]. J Photoch Photobio, A156: 161–170.

Dvoranová D, Brezová V, Mazúra M *et al*., 2002. Investigations of metal-doped titanium dioxide photocatalysts[J]. Appl Catal, B37: 91–105.

Efstathiou A M, Fliatoura K, 1995. Selective catalytic reduction of nitric oxide with ammonia over V_2O_5/TiO_2 catalyst: A steady-state and transient kinetic study[J]. Appl Catal, B6: 35–39.

Farrell A, 2001. Multi-lateral emission trading: lessons from inter-state NO_x control in the United States[J]. Energ Policy, 29: 1061–1072.

Hashimoto K, Wasada K, Osaki M *et al*., 2001. Photocatalytic oxidation of nitrogen oxide over titania-zeolite composite catalyst to remove nitrogen oxides in the atmosphere[J]. Appl Catal, B30: 429–436.

Heck R M, 1999. Catalytic abatement of nitrogen oxides-stationary applications[J]. Catal Today, 53: 519–523.

Ibusuki T, Takeuchi K, 1994. Removal of low concentration of nitrogen oxides through photoassisted heterogeneous catalysis[J]. J Mol Catal, 88: 93–102.

Ichiura H, Kitaoka T, Tanaka H, 2003. Photocatalytic oxidation of NO_x using composite sheets containing TiO_2 and a metal compound[J]. Chemosphere, 51: 855–860.

Kapoor P N, Uma S, Rodriguez S *et al*., 2005. Aerogel processing of MTi_2O_5 (M = Mg, Mn, Fe, Co, Zn, Sn) compositions using single source precursors: synthesis, characterization and photocatalytic behavior[J]. J Mol Catal, A229: 145–150.

Kemp T J, McIntyre R A, 2006. Transition metal-doped titanium(IV) dioxide: Characterisation and influence on photodegradation of poly(vinyl chloride)[J]. Polym Degrad Stabil, 91: 165–194.

Li F B, Li X Z, Ao C H *et al*., 2004. Photocatalytic conversion of NO using TiO_2-NH_3 catalysts in ambient air environment[J]. Appl Catal, B54: 275–283.

Litter M I, Navío J A, 1996. Photocatalytic properties of iron-doped titania semiconductors[J]. J Photoch Photobi, A98: 171–181.

Navío J A, Testa J J, Djedjeian P *et al*., 1999. Iron-doped titania powders prepared by a sol-gel method. Part II: Photocatalytic properties[J]. Appl Catal, A178: 191–203.

Pal B, Sharon M, 2002. Enhanced photocatalytic activity of highly porous ZnO thin films prepared by sol-gel process[J]. Mater Chem Phys, 76: 82–87.

Paola A D, Marci G, Palmisano L *et al*., 2002. Preparation of polycrystalline TiO_2 photocatalysts impregnated with various transition metal ions: characterization and photocatalytic activity for the degradation of 4-nitrophenol[J]. J Phys Chem, B106: 637–645.

Piera E, Tejedor-Tejedor M I, Zorn M E *et al*., 2003. Relationship concerning the nature and concentration of Fe(III) species on the surface of TiO_2 particles and photocatalytic activity of the catalyst[J]. Appl Catal, B46: 671–685.

Radojevic M, 1998. Reduction of nitrogen oxides in flue gas[J]. Environ Pollut, 102: 685–689.

Takeuchi H, Ando M, Kizawa N, 1977. Absorption of nitrogen oxides in aqueous sodium sulfite and bisulfite solutions[J]. Ind Eng Chem Proc Des Dev, 16: 303–308.

Wang H, Wu Z, Zhao W *et al*., 2007. Photocatalytic oxidation of nitrogen oxides using TiO_2 loading on woven glass fabric[J]. Chemosphere, 66: 185–190.

Wu J C S, Cheng Y T, 2006. *In situ* FTIR study of photocatalytic NO reaction on photocatalysts under UV irradiation[J]. J Catal, 237: 393–404.

Yang Y, Li X, Chen J *et al*., 2004. Effect of doping mode on the photocatalytic activities of Mo/TiO_2[J]. J Photoch Photobio, A163: 517–522.

Zhou M, Yu J, Cheng B *et al*., 2005. Preparation and photocatalytic activity of Fe-doped mesoporous titanium dioxide nanocrystalline photocatalysts[J]. Mater Chem Phys, 93: 159–163.

Zhu J, Deng Z, Chen F *et al*., 2006. Hydrothermal doping method for preparation of Cr^{3+}-TiO_2 photocatalysts with concentration gradient distribution of Cr^{3+}[J]. Appl Catal, B62: 329–335.